

Numerical simulation of nonlinear water wave problems

D.C. Lo

Institute of Navigation Science and Technology, National Kaohsiung Marine University, Kaohsiung, Taiwan

Jia-Shen Hu

Department of Shipping Technology, National Kaohsiung Marine University, Kaohsiung, Taiwan

I-Fu Lin

Institute of Navigation Science and Technology, National Kaohsiung Marine University, Kaohsiung, Taiwan

ABSTRACT: The main purpose of present paper aims at the establishment of a numerical model for solving the nonlinear water wave problems. The model is based on the Navier-Stokes equations with the consideration of a free-surface through the streamfunction-vorticity formulation. The main advantage of the streamfunction-vorticity formulation is that pressure field can be eliminated from the Navier-Stokes equations. To demonstrate the model feasibility, the present studies are first concentrated on problems including the collision of two solitary waves with different amplitudes, and the overtaking collision of two solitary waves. Then, the model is also applied to a solitary wave passes over the submerged obstacle in a viscous fluid. Finally, the application of present study is also to simulate the generation of solitary waves by underwater moving object. All examples give very promising results, those applications reveal that present formulation is a very powerful approach to simulate the fully nonlinear water wave problems.

1 INTRODUCTION

The applications of free-surface flows find wide range of navigation science in the design of ship-waves interaction problems. The last one decade have seen growing importance placed on research in free-surface flows simulating. Many analytical methods have been developed to solve traveling and ship-wave problems associated with inviscid fluids as well as for the solution of linear and low order nonlinear problems. Cao and Beck [1] has employed a numerical method to calculate solitary waves generated in an inviscid fluid by a submerged cylinder using the Laplace equation and fully nonlinear free surface boundary conditions. A Taylor-Galerkin method was proposed by Ambrosi and Quartapelle [2] to compute the evolution of water waves with moderate curvature of the free-surface shallow water equations. However, their proposed scheme was extended to study 2D solitary wave passing over a circular cylinder in an inviscid fluid. Lo and Young [3] developed a numerical mode based on velocity-vorticity formulation to solve several free-surface flow problems. The aim of present study is to develop a more general approach to handle inviscid-viscous free-surface flows. When the inviscid model is used, the Poisson-type streamfunction equation and fully-nonlinear free surface boundary conditions are governed for the solution of the free-surface flow. Moreover, it is necessary to deal with viscous free-surface model in order to comprehend the complexities of the phenomenon including the viscous effects. Thus the vorticity transport

equation, Poisson-type streamfunction equation and fully-
-nonlinear free surface boundary conditions should to be solved. The accuracy of the solution for the inviscid-viscous model depends on the representation of actual free surface unknown values.

The numerical treatments of free-surface problems involve the tracking of the moving free-surface boundary during the flow transients. The arbitrary Lagrangian-Eulerian (ALE) coordinate system [4] is used to track the free-surface position on the moving free-surface and the interior computational domain at each time step. It is important to keep the computation of a free-surface position in perspective. In this study, the nodal points can be arbitrarily controlled in order to get finer mesh distribution during computations.

The main difficulty for the solution of the viscous, incompressible free-surface flows indicate that the free-surface boundary conditions are not known priori. In this study, we delivered an accurate and effective scheme based on streamfunction-vorticity formulation and its application to the simulation of wave-wave and wave-structure interaction. In the computational fluid dynamics, the fractional step method is an accurate and efficient scheme for the solution of Navier-Stokes equations. In the present study, the fractional step is used for the discretization of the governing equations and free-surface boundary conditions (FSKBC, FSDBC). The above mentioned of governing flow equations, those equations are coupled and nonlinear, hence an iterative numerical scheme is adopted in order that

we could obtain a significant saving in computer memory.

We present an inviscid-viscous free-surface model using the finite element discretization for the interior of the domain and finite difference discretization for a free-surface. The detailed contents were addressed in the following.

2 MATHEMATICAL FORMULATION

2.1 Incompressible viscous flow

The partial differential equations of the viscous incompressible fluid are governed by the Navier-Stokes equations. The corresponding non-dimensional streamfunction-vorticity form of Navier-Stokes equations in ALE form can be expressed as follows

Streamfunction Poisson equation

$$\nabla^2 \psi = -\omega \quad (1)$$

Vorticity transport equation

$$\frac{\partial \omega}{\partial t} + \left(\frac{\partial \psi}{\partial y} - \hat{u} \right) \frac{\partial \omega}{\partial x} + \left(-\frac{\partial \psi}{\partial x} - \hat{v} \right) \frac{\partial \omega}{\partial y} = \frac{1}{\text{Re}} \nabla^2 \omega \quad (2)$$

where ψ is the streamfunction, ω is the vorticity, Re is the Reynolds number, (\hat{u}, \hat{v}) is the mesh velocity in the x, y direction, respectively.

Equations (1) and (2) are known as the Navier-Stokes equations in streamfunction-vorticity form. We seek a solution in the domain Ω , which satisfies the initial conditions, with no-slip or slip velocity boundary conditions depending on the need on the solid boundary Γ of Ω .

2.2 Boundary conditions

Consider a two-dimensional, viscous and incompressible fluid. In the present study, the free-surface flow is considered as a two-phase flow. It is assumed that the adjacent fluids are impermeable at the interface with constant density and viscosity. The main difficulty of the free-surface flow is that the position of the free-surface boundary is not known *a priori*. The boundary-fitted coordinates system is used to solve the equations for the free-surface boundary conditions in streamfunction-vorticity form. The relationships among velocity, streamfunction and vorticity can be defined as $(u, v) = (\psi_y, -\psi_x)$, $\omega = v_y - u_x$. The arbitrary physical space (x, y) can be general mapped to a normalized computational domain (ξ, η) with the help of the boundary-fitted coordinates system.

According to the statement of a material surface, a particle on the surface must remain on the surface

itself. By satisfying the above kinematic condition in an arbitrary frame of reference to be

$$h_t = v - (u - \hat{u})h_x \quad (3)$$

In the above equation, the frame of reference moves with a free surface in the vertical direction and \hat{u} is either zero or equal to u .

The free surface dynamic boundary condition (FSDBC) represents the continuity of the stresses on the free-surface and is obtained by force balance equations. Neglecting the surface tension effect on the free-surface, the FSDBC in an arbitrary frame of reference can be obtained by combining momentum equations to yield

$$\begin{aligned} & (u_t + (u - \hat{u})u_x + (v - \hat{v})u_y - \frac{1}{\text{Re}}(u_{xx} + u_{yy}))x_\xi + \\ & (v_t + (u - \hat{u})v_x + (v - \hat{v})v_y + \frac{1}{F_r^2} - \frac{1}{\text{Re}}(v_{xx} + v_{yy}))y_\xi = 0 \end{aligned} \quad (4)$$

As far as initial condition is concerned, an initial solitary wave is imposed as present in Gtimshaw's third order formulas [5] in the free-surface profile and streamfunction.

3 NUMERICAL FORMULATION

For the solution of 2D free-surface flow using streamfunction-vorticity formulation, the quadrilateral finite element is used to discretize the Poisson-type streamfunction equation and the vorticity transport equation. The free-surface boundary conditions are solved by the FDM.

Table 1. Comparison of present and Su and Mirie results [6] of the maximum amplitude run-up during the collision

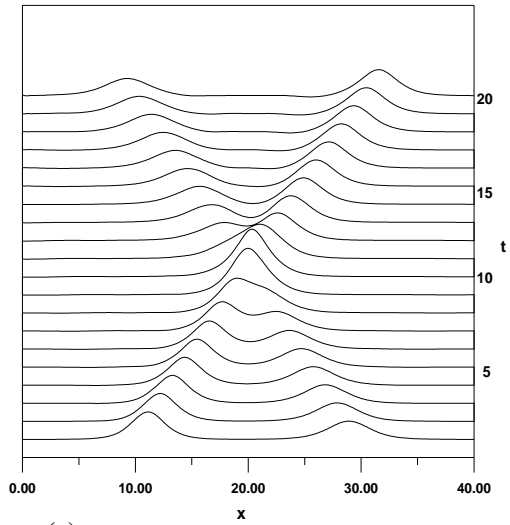
A, B	0.2,0.2	0.3,0.2	0.4,0.2	0.5,0.2	0.6,0.2
Present	0.4298	0.5436	0.6604	0.7866	0.9420
Su and Mirie	0.4240	0.5375	0.6520	0.7675	0.8840
Error (%)	1.37	1.13	1.29	2.49	6.56

4 RESULTS AND DISCUSSIONS

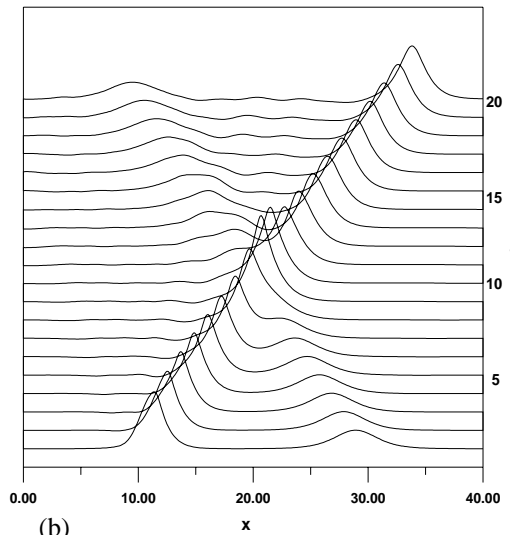
4.1 Validation of the numerical model for two solitary waves head-on collision

It is interesting to note that the solitary waves which retain their identity upon collision are called solitons. The topics of solitons had a large impact on various branches of modern physics, and this topic attracts many investigators to study. In this section, the results for collisions of two opposite solitary waves using the present numerical scheme were

verified. Su & Mirie [6] study the head-on collisions of two solitary waves generated using a perturbation method. The flow is an inviscid and incompressible fluid. In a similar work, Mirie & Su [7] depicted the collisions of two solitary waves to confirm the existence of a secondary wave as predicted in their previous work.



(a)



(b)

Fig. 1. Evolution of free surface position of different amplitudes. (a) $A = 0.3, B = 0.2$ (b) $A = 0.6, B = 0.2$

We consider the collision of two solitary waves with different amplitudes. Calculations were carried out for initial heights of a solitary wave at the left-hand side given by the expression, $A_0 = 0.2, 0.3, 0.4, 0.5, 0.6$. The initial amplitude of a solitary wave at the right-hand side was assumed to be equal to 0.2. The grid size was $\Delta x = 0.1, \Delta t = 0.02$ and the range consisted of 8000 quadrilateral elements. The Reynolds number is $Re = 60,000$ for this case. In this moving grid, the interval of Δx is fixed but Δy is changed by the FSKBC. The maximum amplitudes of the head-on collision of two solitary waves were shown in Table 1. Good agreement with the solution obtained by Su & Mirie [6] was depicted in above

table. Table 1 provides the list of 5 values that were computed for verifying the model in this study. The present numerical model could predict the maximum run-up with less than 2% error in the cases of $A = 0.2, 0.3, 0.4$ and $B = 0.2$. However, the error turned out to be a 6.56% at $A = 0.6, B = 0.2$. A partial explanation for this may lie in the fact that the computation of present case the fully nonlinear boundary conditions are considered. However, the result obtained by Su & Mirie [6] was to assume the weakly nonlinear effect on the free surface for this case. Figure 1 shows the evolution of free surface profiles of the two solitary waves during the collisions. The high nonlinear interaction has been observed during the collisions between the two solitary waves. We also found that after the collision, the solitary waves recuperate almost all of their original amplitudes in the time range of the transient. Also, the solitary waves have experienced phase change and were trailed by a dispersive wave train when the two solitary waves head-on collide in our computation.

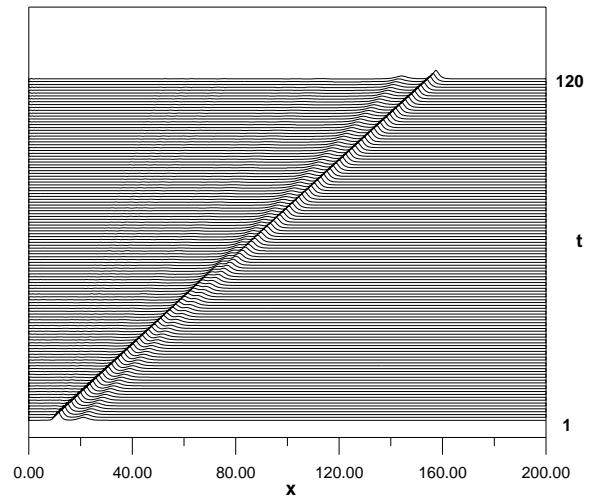


Fig. 2. Evolution of free surface position of different amplitudes. ($A = 0.6, B = 0.2$)

4.2 The overtaking collision of two solitary waves

As mentioned before of head-on collision of two solitary waves, now we consider the simulation of the 2D overtaking of two solitary waves of amplitudes 0.6, 0.2. The initial amplitudes of the two solitary waves were assumed to be equal to 0.6 on the left-hand side and 0.2 on the right-hand side. The positions of the two solitary waves were initially fixed at $x = 10$ and $x = 20$ in the same direction. The present simulation of free-surface flow was tested for inviscid model. In the present computations, the non-dimensional parameter with finite depth, D equal to 1 and length in the x -direction equal to 200 were assumed, respectively. A total number of 16,000 elements and 17,017 nodes

(1001, 17 divisions in the x -, y -directions, respectively) with a time step $\Delta t=0.02$ were used for computation in the present case. Figure 2 depict the time evolution of the interaction of two solitary waves. The highly nonlinear behavior during the overtaking process between two opposite solitary waves is presented in Figure 2. However, both solitary waves emerge completely unscathed.

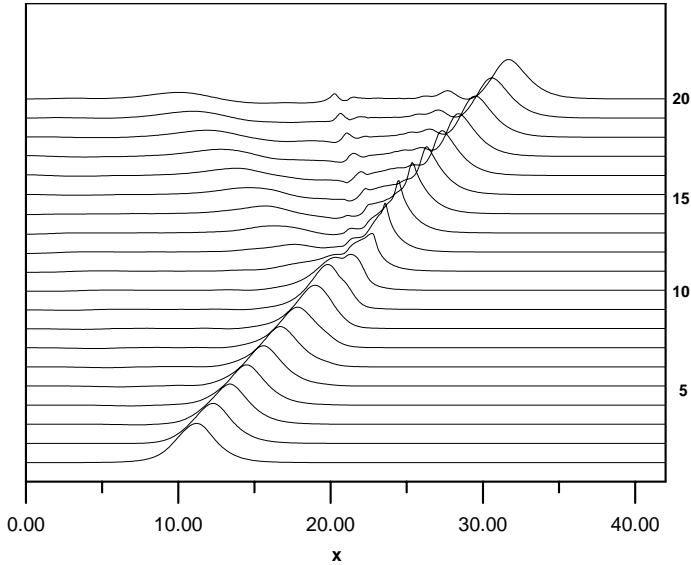


Fig. 3. Evolution of free surface elevation at different time for $Re = 60,000$

4.3 Solitary wave passing over a submerged structure

The computation for a fluid-structure interaction with a free-surface was carried out for a solitary wave passing through the submerged structure. We assume the dimensionless length of the mean water level as 1 and length as 42 as well as initial amplitude of the solitary wave as 0.4. The initial condition of a solitary wave was fixed in $x=10$ of the water channel. The flow was considered to be viscous. For the present case of viscous model, the fluid is assumed to have small viscosity ($Re=60,000$, $Fr=1$), our goal is the observation of the separated flow pattern for the viscous model. Figure 3 lists the time evolution of a solitary wave passing through the submerged structure in present simulation.

In order to plot the vortex motion generated during wave-structure interactive process. The streamline were plotted and were shown in Figure 4. The local velocity distribution near the structure was given in Figure 5. The gradual development of the recirculating flow regimes at the downstream of the structure and was clearly predicted by the present numerical study. The recirculating flow generated at the trailing edge of the structure was clearly observed in Figure 5. The results reflected in Figure

5 indicate that the viscosity plays an important role to affect the interactive processes between the solitary wave and the solid structure. In general, the vortical flow is always grown up on the rear surface of the structure while the solitary wave passes through the submerged structure in viscous fluid.

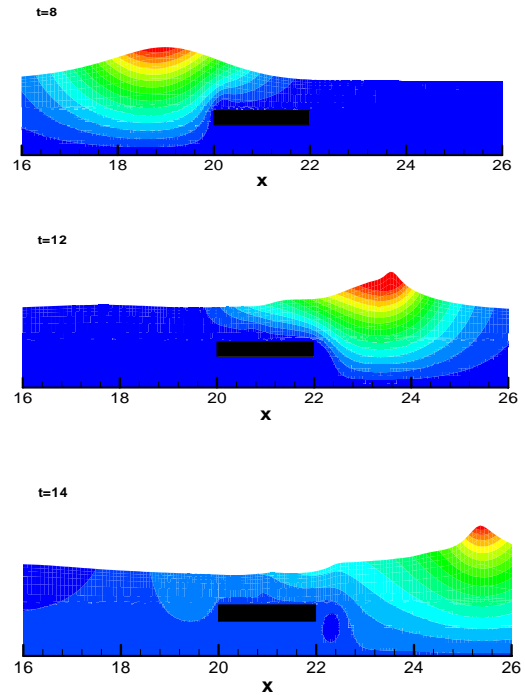
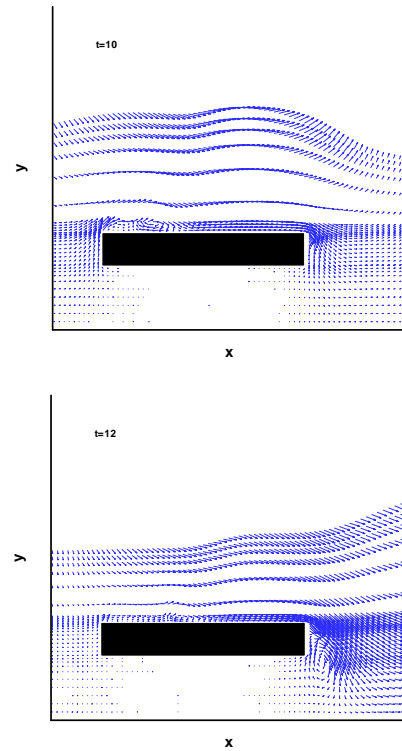


Fig. 4. Evolution of streamline distribution at different time



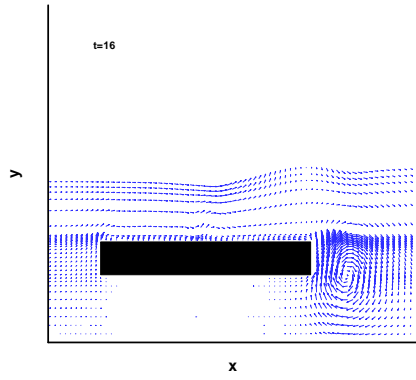


Fig. 5. Local velocity distribution at different time

4.4 The generation of solitary wave by underwater moving object

The final test case illustrates the capability of 2D free surface algorithm for a succession of solitary waves generated by underwater moving object. The submerged object is moving with a constant velocity in the negative x-coordinate direction in shallow water. The layout of geometry and conditions is well illustrated in Figure 6. We assume the constant velocity of underwater object is moving in a channel $[0,70] \times [0,1]$ with the object as shown in Figure 6, initially the region of object is

$$b(x, y) = \begin{cases} B_{\max} \cos^2 \left\{ \frac{\pi}{L} (x - 40) \right\}, & -\frac{L}{2} < (x - 40) < \frac{L}{2} \\ 0, & \text{otherwise} \end{cases} \quad (5)$$

For the case of present used study, we assume $B_{\max} = 0.15$ and $L = 1$. The computation for a submerged moving object in a channel is assumed to be 70 in the x direction and with the upstream dimensionless depth of 1 in the y direction. The computation of the present case is used with a total number of 9,600 elements and 10,217 nodes with a time step $\Delta t = 0.02$ and $Re = 30,000$. Figure 7 depicts the local velocity and vorticity distributions at $t = 100$ for the flow past the submerged object. The flow circulation behind the object is seen in Figure 7, in which the region of the vortex structure near the object is delineated. Further, the streamline contours at different time are also revealed in figure 8. Finally, the evolution of free surface elevation at different time for the propagation of solitary waves is shown in figure 9. It can be observed that the generation and propagation of the upstream advancing solitary wave become more dominated as time increases.

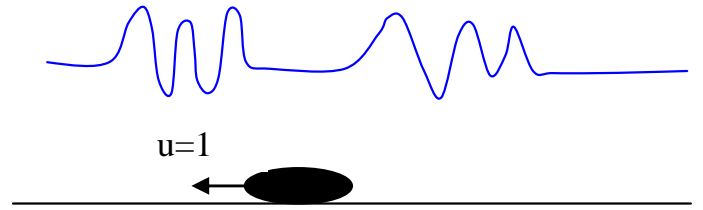


Fig. 6. Layout of an underwater moving object

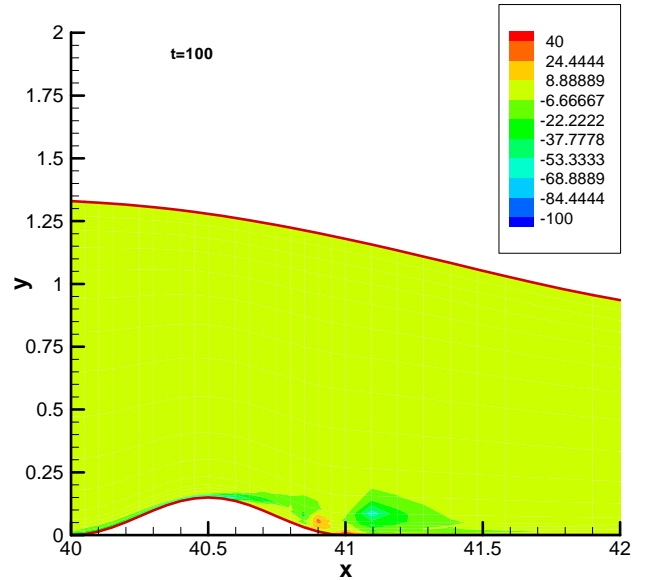
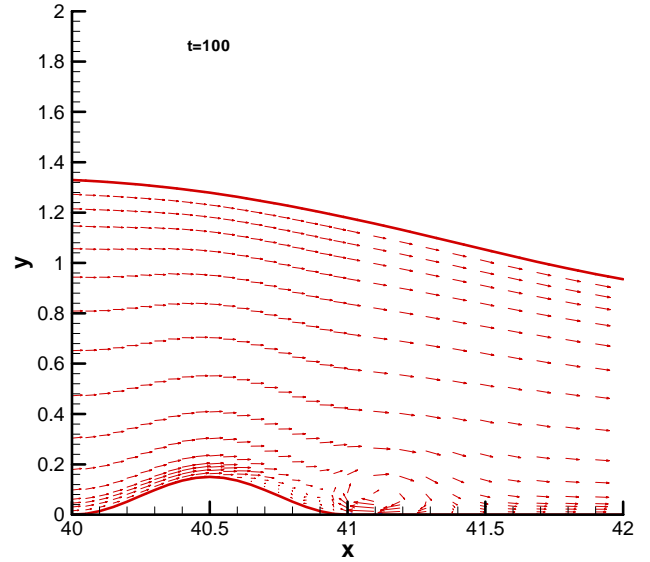


Fig. 7. Local velocity and vorticity distribution at $t = 100$

5 CONCLUSIONS

A numerical model by combing FEM and FDM for free-surface flow problems was proposed using the Navier-Stokes equations in streamfunction-vorticity form. The present study has extended to an inviscid-

viscous model for free surface flow problems. The accuracy of results obtained we have is excellent. Also, both inviscid and viscous models play an important role to free surface flows. However, the key issue in the viscous model is to find the accurate solution for separated flow pattern of a solitary wave passing over the submerged structure. It shows that the streamfunction-vorticity formulation gives accurate and correct results for flow problems with a free surface. We can conclude with certainty that both inviscid and viscous models are able to simulate non-linear water waves in present work.

6 ACKNOWLEDGMENTS

The work reported in this chapter was supported by the National Science Council, Taiwan under the grant no. 95-2221-E-022-020. It is greatly appreciated.

REFERENCES

- [1] Y. Cao and R.F. Beck, Numerical computations of two-dimensional solitary waves generated by moving disturbances, *Int. J. Numer. Meth. Fluids*, 17 (1993) 905-920.
- [2] D. Ambrosi and L. Quartapelle, A Taylor-Galerkin method for simulating nonlinear dispersive water waves, *J. Comput. Phys.*, 146 (1998) 546-569.
- [3] Lo, D.C., and Young, D. L. (2004). "Arbitrary Lagrangian-Eulerian finite element analysis of free surface flow using a velocity-vorticity formulation." *J. Comput. Phys.*, 195, 175-201.
- [4] C.W. Hirt, A.A. Amsden and J.L. Cook, An arbitrary Lagrangian Eulerian computing method for all flow speeds, *J. Comput. Phys.*, 14 (1974) 227-253.
- [5] R. Grimshaw, The solitary wave in water of variable depth, part 1. *J. Fluid Mech.* 46 (1971) 611-622.
- [6] C.H. Su and R.M. Mirie, On head-on collision between two solitary waves, *J. Fluid Mech.* 98 (1980) 509-529.
- [7] R.M. Mirie and C. H. Su, Collisions between two solitary waves, Part 2: A Numerical Study, *J. Fluid Mech.* 115 (1982).

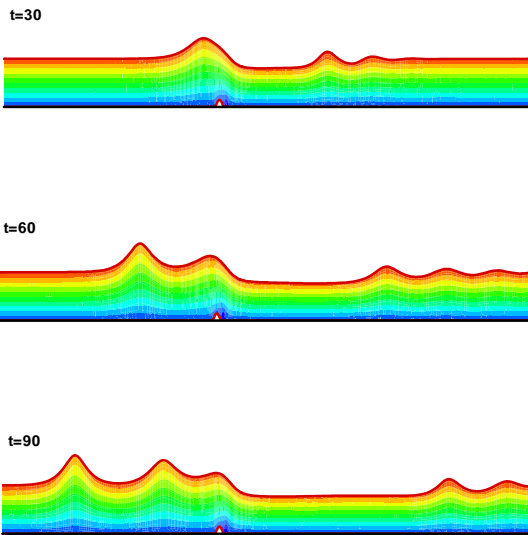


Fig. 8. Streamline distributions at different time

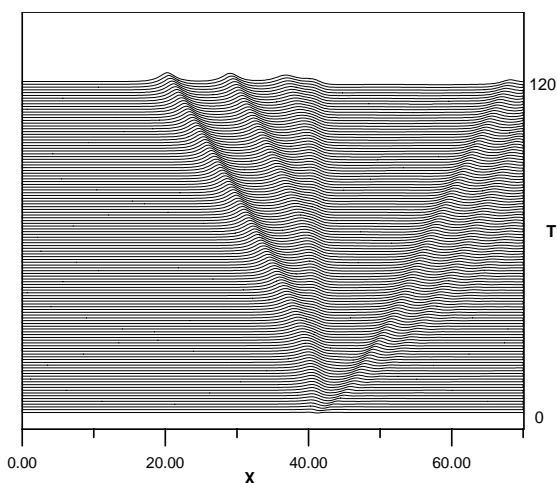


Fig. 9. The evolution of free surface elevation at different time